

Cage Compounds

Homochiral Self-Sorted and Emissive Ir^{III} Metallo-CryptophanesVictoria E. Pritchard,^[a] Diego Rota Martir,^[b] Samuel Oldknow,^[a] Shumpei Kai,^[c]
Shuichi Hiraoka,^[c] Nikki J. Cookson,^[a] Eli Zysman-Colman,^{*,[b]} and Michael J. Hardie^{*,[a]}

In memory of Dr. Julie Fisher

Abstract: The racemic ligands (±)-tris(isonicotinoyl)-cyclo-triguiacylene (L1), or (±)-tris(4-pyridyl-methyl)-cyclo-triguiacylene (L2) assemble with racemic (Λ,Δ)-[Ir(ppy)₂(MeCN)₂]⁺, in which ppy = 2-phenylpyridinato, to form [Ir(ppy)₂]₃(L)₂³⁺ metallo-cryptophane cages. The crystal structure of [Ir(ppy)₂]₃(L1)₂·3BF₄ has *MM*-ΛΛΛ and *PP*-ΔΔΔ isomers, and homochiral self-sorting occurs in solution, a process accelerated by a chiral guest. Self-recognition between L1 and L2 within cages does not occur, and cages show very slow ligand exchange. Both cages are phosphorescent, with [Ir(ppy)₂]₃(L2)₂³⁺ having enhanced and blue-shifted emission when compared with [Ir(ppy)₂]₃(L1)₂³⁺.

Metallo-cages are discrete 3D-coordination assemblies with a hollow interior and have applications as hosts and nanoscale vessels.^[1] They form through the self-assembly of multidentate ligands with metals, or with metal complexes with controlled available coordination sites ("metallo-tectons"). Luminescent metallo-cages are known,^[2–6] with most examples exhibiting fluorescence-active ligands,^[2] alongside rarer examples of cages with pendant metal-complex emissive groups.^[3] There are very few examples of metallo-cages constructed from inherently phosphorescent structural components.^[4–6] Cyclometalated Ir^{III} complexes bearing either two N-donor ligands or one NN chelating ligand represent an important subclass of

phosphorescent materials.^[7] Lusby and co-workers reported the enantiopure Ir^{III} metallo-cage [Ir(ppy)₂]₆(tcb)₄·(OTf)₆ (tcb = 1,3,5-tricyanobenzene),^[4] which self-assembles, despite the inertness of the d⁶ Ir^{III} centre, as the *C,C-cis-N,N-trans* arrangement of the ppy ligands has a *trans*-labilising effect. The cage shows red-shifted emission compared with a monomeric analogue, and enhanced photoluminescence quantum yields (Φ_{PL}). To date, this is the only report of a 3D metallo-cage that utilizes [Ir(ppy)₂] as the sole metal centre, although mixed metal examples are known.^[5]

Here, we report two metallo-cages of the type [Ir(ppy)₂]₃(L)₂³⁺, in which L is a chiral tripodal ligand related to the molecular host cyclotrimeratrylene (CTV). [M(chelate)]₃L₂ cages with CTV-type ligands are known as metallo-cryptophanes, and most examples feature square planar metals.^[8] The [Ir(ppy)₂]₃(L)₂³⁺ cages reported here show homochiral sorting on crystallization and in solution, and slow ligand exchange behaviour is observed.

Cages [Ir(ppy)₂]₃(L1)₂³⁺ **1** and [Ir(ppy)₂]₃(L2)₂³⁺ **2** are formed from nitromethane mixtures of (Λ,Δ)-[Ir(ppy)₂(MeCN)₂]⁺X (X = PF₆⁻, BF₄⁻) and (±)-L1 or (±)-L2 in 3:2 stoichiometry (Scheme 1). Electrospray ionization mass spectrometry (ESI-MS) gives a triply charged *m/z* peak at 983.1120 (cage **1**) or at 955.2853 (cage **2**), along with [Ir(ppy)₂]₃(L)₂³⁺ and [Ir(ppy)₂]₂(L)₂³⁺ fragment species (Figures S3 and S4 in the Supporting Information). Initial ¹H NMR spectra of [Ir(ppy)₂(NCMe)₂]⁺X and L in [D₃]-MeNO₂ show considerable broadening of the resonances and chemical shift changes, most saliently the ppy protons *ortho* to the coordinating N (H_A) and C (H_H) move upfield and downfield, respectively. For cage **2**, the previously sharp CH₂ bridge singlet of L2 at 5.19 ppm becomes a complex multiplet as free rotation is hindered (Figure S15). ROESY spectra of **1** and **2** give the expected couplings, including between H_H on the ppy ligands and the *ortho* pyridyl protons of L (Figures S8 and S16). Diffusion ordered NMR spectroscopy in [D₃]-MeNO₂ for 1·3PF₆ (Figure S9) gave a hydrodynamic radius of 18.99 Å.

The structure of 1·3BF₄·*n*(MeNO₂) was confirmed by crystallography (Figure 1).^[9] There are two independent cage **1** cations that show minor structural differences. Anions and additional solvent were not located due to significant disorder. Each cage has three pseudo-octahedrally coordinated Ir^{III} centres, each with two ppy ligands and the pyridyl groups from two L1 ligands are in a *cis* arrangement. The two L1 ligands bridge between three Ir^{III} centres. The average torsion angle between *cis*-pyridyl groups is 38.04°, typical for [Ir(ppy)₂(pyridyl)₂]-type

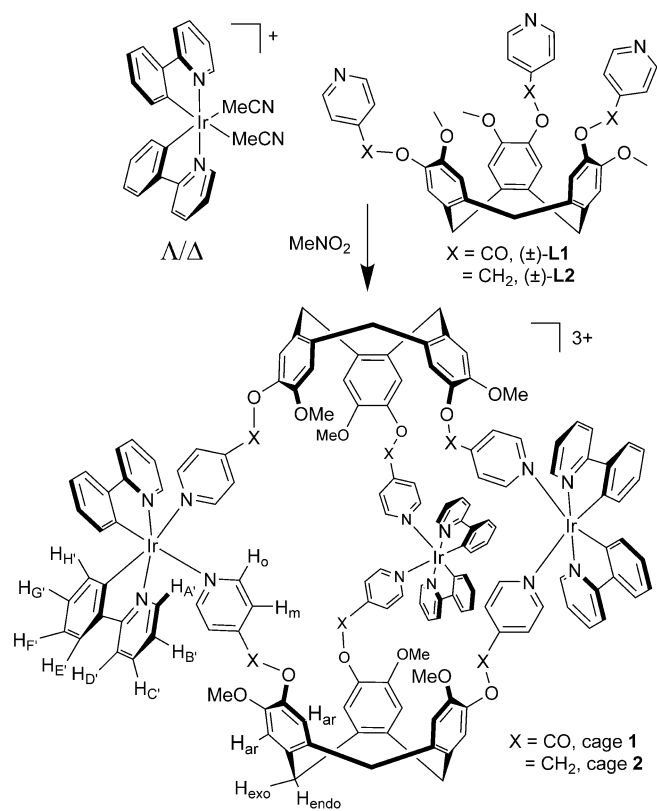
[a] Dr. V. E. Pritchard, S. Oldknow, Dr. N. J. Cookson, Prof. M. J. Hardie
School of Chemistry, University of Leeds
Woodhouse Lane, Leeds LS2 9JT (UK)
E-mail: m.j.hardie@leeds.ac.uk

[b] D. Rota Martir, Dr. E. Zysman-Colman
Organic Semiconductor Centre, EaSTCHEM School of Chemistry
University of St Andrews
St Andrews, Fife KY16 9ST (UK)
E-mail: eli.zysman-colman@st-andrews.ac.uk

[c] S. Kai, Prof. S. Hiraoka
Department of Basic Science, Graduate School of Arts and Sciences
The University of Tokyo
3–8-1 Komaba, Meguro-ku, Tokyo 153-8902 (Japan)

Supporting information and the ORCID number(s) for the author(s) of this article can be found under <https://doi.org/10.1002/chem.201701348>. Additional data are also available under <https://doi.org/10.5518/181>.

© 2017 The Authors. Published by Wiley-VCH Verlag GmbH & Co. KGaA. This is an open access article under the terms of the Creative Commons Attribution License, which permits use, distribution and reproduction in any medium, provided the original work is properly cited.



Scheme 1. Synthesis of metallo-cryptophane cage species.

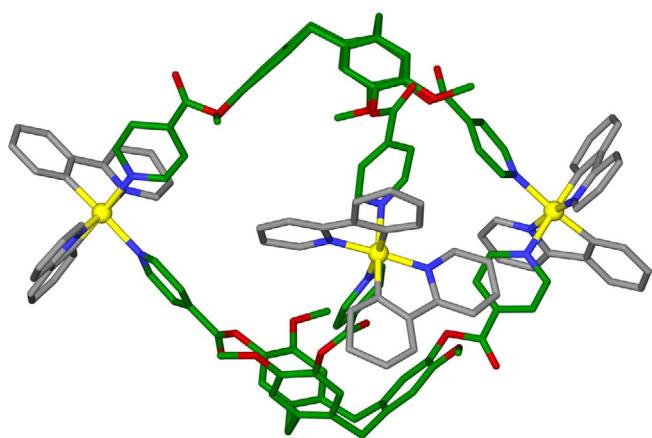


Figure 1. A $[\text{Ir}(\text{ppy})_2(\text{L}1)_2]^{3+}$ cage from the crystal structure of $1\cdot 3\text{BF}_4\cdot n(\text{CH}_3\text{NO}_2)$; L1 and ppy ligands shown in green and grey, respectively.

complexes^[10] with the bowl shape of CTV-type ligands being able to accommodate these torsion angles within the cage structure.

Both L1 ligands within each cage 1 are the same enantiomer, giving the chiral *anti*-cryptophane isomer. Each $[\text{Ir}(\text{ppy})_2]$ unit within a cage has the same chirality, such that only the enantiomeric *MM*- $\Delta\Delta\Delta$ and *PP*- $\Delta\Delta\Delta$ cage isomers are observed in the structure. Given that the Δ and Δ enantiomers of the $[\text{Ir}(\text{ppy})_2]^+$ moieties and the *M* and *P* enantiomers of the L-types ligands are present in the reaction mixture, there are twelve possible stereoisomers of the cage. The ^1H NMR spectra

of both cages 1 and 2 undergo significant sharpening upon standing (Figures S7 and S15 in the Supporting Information), and fully equilibrate after several months. The ^1H NMR spectrum of cage $1\cdot 3\text{PF}_6$, collected after 3 months of standing, is virtually identical to that of the single crystals of $1\cdot 3\text{BF}_4\cdot n(\text{CH}_3\text{NO}_2)$ re-dissolved in $[\text{D}_3]\text{-MeNO}_2$ (Figure 2a,b). $(\pm)\text{-L1}$ was resolved into its constituent enantiomers by chiral HPLC,^[11] and each L1 enantiomer reacted with each of $\Delta\text{-}[\text{Ir}(\text{ppy})_2(\text{MeCN})_2]\cdot\text{BF}_4$ and $\Delta\text{-}[\text{Ir}(\text{ppy})_2(\text{MeCN})_2]\cdot\text{BF}_4$. As expected, the

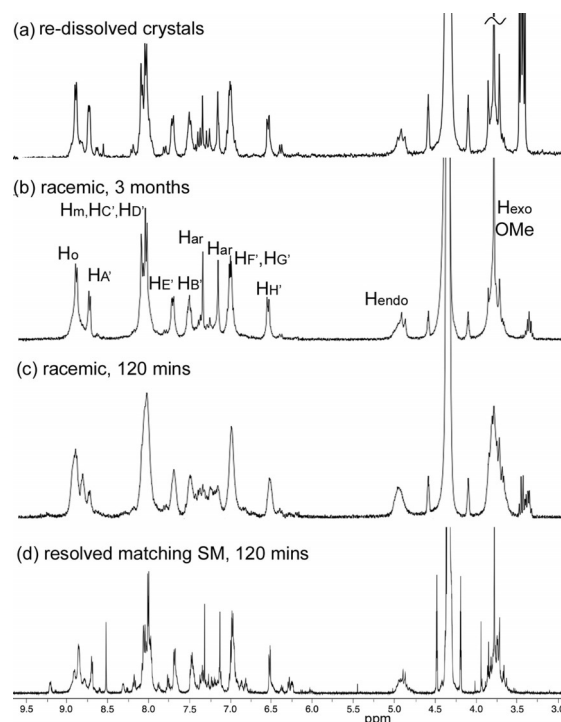


Figure 2. ^1H NMR spectra in CD_3NO_2 of (a) re-dissolved racemic single crystals of *MM*- $\Delta\Delta\Delta$ and *PP*- $\Delta\Delta\Delta$ cages of $1\cdot 3\text{BF}_4$; (b) $(\Delta, \Delta)\text{-}[\text{Ir}(\text{ppy})_2(\text{MeCN})_2]\cdot\text{PF}_6$ and $(\pm)\text{-L1}$ 3 months after mixing; (c) $(\Delta, \Delta)\text{-}[\text{Ir}(\text{ppy})_2(\text{MeCN})_2]\cdot\text{PF}_6$ and $(\pm)\text{-L1}$ 2 hrs after mixing; (d) matched pair of $\Delta\text{-}[\text{Ir}(\text{ppy})_2(\text{MeCN})_2]^+$ and one L1 enantiomer after 2 hrs.

two combinations that were mis-matched pairs of enantiomers gave poorly resolved ^1H NMR spectra (Figures S10 and S11), whereas the two combinations that were matched pairs (presumably *M*- Δ and *P*- Δ) gave sharp spectra in short timeframes that were similar to the fully sorted cage mixture (Figures 2d, S12, S13). ESI-MS of matched and mis-matched pairs are similar with all combinations showing cage formation (Figure S14). The observed ^1H NMR spectral sharpening is therefore indicative of equilibration involving chiral self-sorting of an initial mixture of cage stereoisomers; this was also seen in our previous studies of a $[\text{Pd}_6(\text{L}1)_8]^{12+}$ cage but only the ligand was a chiral component.^[12] We could not resolve the sorted cages by analytical chiral HPLC.

Homochiral metallo-cages with tris-chelate metal coordination are known both from achiral^[13a,b] and resolved chiral ligands.^[13c-e] Metallo-cages that show homochiral self-sorting from a racemic mixture of ligand enantiomers observed in so-

lution are rare,^[14] although these include Pd^{II} metallo-cryptophanes.^[8a] The simultaneous chiral self-sorting of both ligand and pre-formed inert metallo-tecton as reported here have not been previously reported. In a preliminary investigation of the influence of chiral guests on the self-assembly of cage 1, globular additives were included in 3:2 mixtures of (Λ,Δ)-[Ir(ppy)₂(MeCN)₂]⁺PF₆⁻ and (\pm)-L1. Addition of chiral *R*-camphor or *S*-camphor led to noticeably faster sharpening of the ¹H NMR spectra than in their absence, but this was not observed for the addition of achiral adamantane (Figures S15–S20 in the Supporting Information). Interestingly, addition of the related anionic species *R*-(or *S*)-10-camphorsulfonic acid to the reaction mixture prevents cage formation presumably as carboxylate is a competing ligand for the iridium (Figures S21 and S22).

The cages do not show self-recognition of L-ligand species. ESI-MS of a MeNO₂ solution of L1, L2 and [Ir(ppy)₂(MeCN)₂]⁺BF₄⁻ shows a statistical mixture of 1:[Ir(ppy)₂]₃(L1)(L2)]³⁺:2 cage species (Figure 3). Mixing 1:3BF₄ and 2:3BF₄ in MeNO₂ results in very slow exchange between L1 and L2 with appreciable ligand exchange only observed after four weeks, and near-statistical mixing reached after ten weeks (Figure S6 in the Supporting Information). Thus, these cages have a high degree of kinetic stability but are not completely inert. It is interesting to note that this speciation behaviour is in contrast with recently reported [Pd₃L₂]⁶⁺ metallo-cryptophanes, which exclusively formed homocages from two different L-type ligands, with no ligand exchange.^[8a]

The absorption spectra of 1 and 2 in dichloromethane (DCM) are similar to other [Ir(ppy)₂(NN)]⁺ systems,^[7] and characterised by two intense ligand centred (¹LC) transitions between 260 and 320 nm localised on the ppy and three lower intensity broad bands below 380 nm that consist of spin-allowed and spin-forbidden mixed metal-to-ligand and ligand-to-ligand charge transfer (¹MLCT/¹LLCT and ³MLCT/³LLCT, respectively) transitions (Figure S26 in the Supporting Information). The weak CT transition observed for 1 at 470 nm was not reported for the monomeric [Ir(ppy)₂(4-pyCO₂Et)₂]⁺ (4-pyCO₂Et = 4-ethyl isonicotinate),^[10c] suggesting increased conjugation in 1 due to the CTV scaffold. For both 1 and 2, the excitation spectra in DCM match the absorption spectra and indicate a single photophysically active species.

Cages 1 and 2 are emissive in DCM solution and in the solid state. Upon photoexcitation of 1, a broad and unstructured

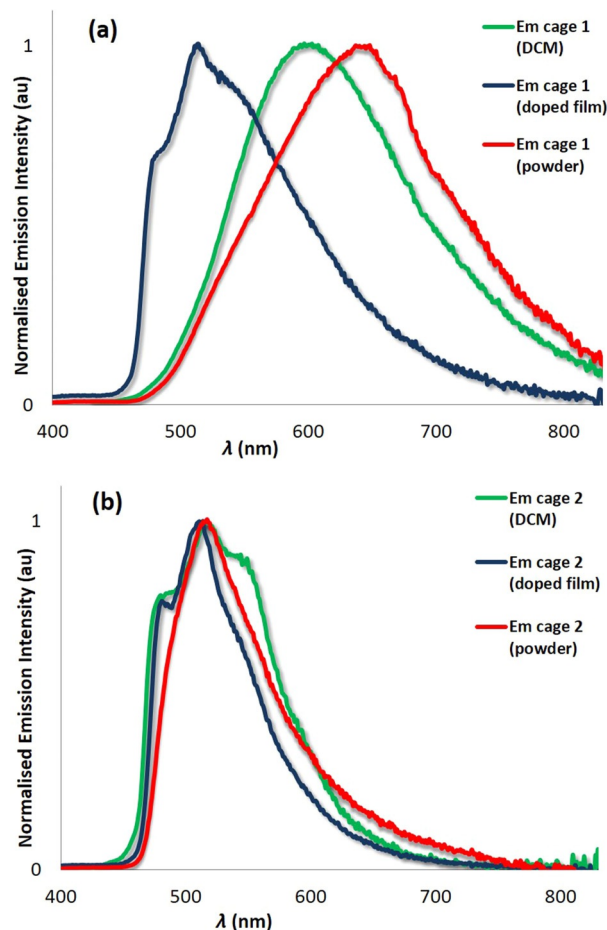


Figure 4. Normalised photoluminescence spectra of a) 1:3BF₄ and b) 2:3BF₄. Green lines are de-aerated DCM solutions; blue lines are PMMA-doped films with 5 wt% of cages spin-coated on a quartz substrate; red lines are bulk powders.

emission is observed both in DCM and in the powder (Figure 4a) due to emission from a mixed ³MLCT/³LLCT state.^[7] The photoluminescence spectrum in the powder is red-shifted ($\lambda_{\text{max}} = 648$ nm) compared to that in DCM ($\lambda_{\text{max}} = 604$ nm); however, 1 possesses similarly low Φ_{PL} of around 1% and bi-exponential decay kinetics in both media (Table 1). Due to the increased conjugation into the CTV scaffold, cage 1 shows red-shifted emission and similar Φ_{PL} compared to [Ir(ppy)₂(4-

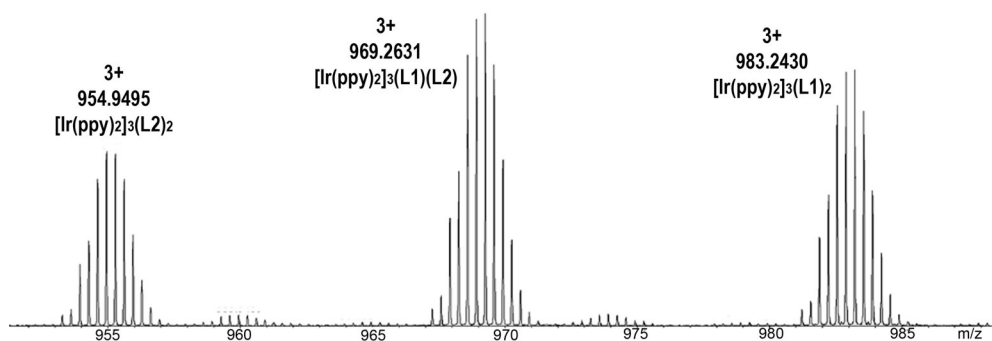


Figure 3. ESI-MS of a 1:1:3 mixture of L1:L2:[Ir(ppy)₂(MeCN)₂]⁺BF₄⁻ in MeNO₂ showing formation of a statistical mixture of homoleptic and heteroleptic cages.

Table 1. Photophysical properties of complexes **1-3**(BF₄) and **2-3**(BF₄).

Entry	λ_{em} (nm)			Φ_{PL} (%) ^[d]			τ_e (ns) ^[g]		
	DCM ^[a,b,f]	Film ^[c,f]	Powder	DCM ^[a]	Film ^[c,e]	Powder ^[e]	DCM ^[a]	Film ^[c]	Powder
1	604	481	648	1	5.5	1.3	59	634	55 (0.6)
		(0.7)					(0.7)	(0.4)	
		514					129	2319	203
		(1)					(0.3)	(0.6)	(0.4)
		556							
		(0.8)							
2	485	486	519	15	10	1.6	523	688	141
		(0.8)					(0.4)	(0.7)	(0.4)
		516 (1)					887	3042	1175
		(1)					(0.6)	(0.3)	(0.6)
		547							
		(0.6)							
		545							
		(0.6)							

[a] Measurements in degassed DCM at 298 K. [b] Quinine sulfate employed as the external reference (Φ_{PL} = 54.6% in 0.5 M H₂SO₄ at 298 K). [c] PMMA-doped films (5 wt% of cage) formed by spin-coating deposition on a quartz substrate. [d] Φ_{PL} measurements were carried out under nitrogen (λ_{exc} = 360 nm). [e] Values obtained using an integrating sphere. [f] Principal emission peaks listed with values in parentheses indicating relative intensity. [g] λ_{exc} = 378 nm; values in parentheses are pre-exponential weighting factors, in relative % intensity, of the emission decay kinetics.

pyCO₂Et)₂)⁺ (λ_{max} = 560 nm; Φ_{PL} = 2%).^[10c] Lusby's [Ir(ppy)₂]₂(tcb)₄)⁶⁺ cage also showed a red-shifted emission (λ_{max} = 575 nm) when compared with the corresponding [Ir(ppy)₂(NCPH)₂]OTf complex (λ_{max} = 525 nm); however, unlike for cage **1** and other Ir(ppy)₂ discrete supramolecular systems,^[15] the Φ_{PL} for the Lusby cage was enhanced compared with that of the mononuclear complex (Φ_{PL} = 4% vs. Φ_{PL} = < 1%).^[4]

To mitigate non-radiative vibrational motion in the cage, we spin-coated 5 wt% of **1** in polymethyl methacrylate (PMMA), which serves as an inert matrix. The emission in the thin film was blue-shifted and more structured (λ_{max} = 514 nm) compared to both the powder and solution spectra. The Φ_{PL} of 5.5% was enhanced as a result of the rigidity conferred by the PMMA host and the emission lifetimes were significantly longer (τ_e = 634 and 2319 ns).

The photoluminescence spectrum of cage **2** in DCM is more structured and blue-shifted (λ_{max} = 516 nm) compared to **1**, indicating an emission that is more predominantly ligand-centred (³LC; Figure 4b). The blue-shifted emission of **2** compared to **1** was expected considering the presence of the electron-withdrawing ester moieties located on L1 in **1**, which stabilise the LUMO.^[10c] Cage **2** shows a significantly enhanced Φ_{PL} and longer τ_e compared to **1** in DCM (Φ_{PL} = 15%, τ_e = 523, 887 ns).

Unlike **1**, the emission of **2** as a powder is not significantly red-shifted (λ_{max} = 519 nm), though the emission profile is less structured, showing less well-resolved vibrational bands as shoulders of the main emission peak. The emission profile for **2** in the PMMA-doped thin film is likewise very similar to that in DCM. Although Φ_{PL} values are low in the powder (Φ_{PL} = 1.6%), in the doped film they are higher (Φ_{PL} = 10%). Emission lifetimes are expectedly longer in doped films than in powder (Table 1). Attempts to synthesize an analogous mononuclear complex of 4-phenoxyethylpyridine for comparison were not successful due to ligand oligomerization.

In summary, phosphorescent [Ir(ppy)₂]₂(L)₂)³⁺ metallo-cryptophanes can be synthesized in high yields, with the CTV-type ligands being able to accommodate torsion angles typical of [Ir(ppy)₂(L)₂] complexes to form rare examples of 3D Ir^{III} cyclometallated coordination cages. These cages undergo ligand exchange processes over months and show a remarkably high degree of homochiral self-sorting of both ligand and metallo- tecton, but not self-recognition between similar L-type ligands. Chiral sorting is enhanced by the presence of neutral chiral additives. For cage **1**, chiral self-sorting occurs relatively rapidly upon crystallisation through an induced seeding effect, but on a timescale of months in solution. Luminescence properties of the two cages are quite distinct, pointing to an ability to tune the photophysical properties of these systems. Cage **2** showed an enhanced and blue-shifted emission compared to **1**, reaching a Φ_{PL} of 15% in DCM solution and 10% in doped film. These are promising systems for a variety of applications including semiochemical hosts, photoredox catalysts and in energy conversion materials.

Acknowledgements

We thank the EPSRC (DTG award 1238852, EP/K039202/1, EP/M02105X/1, EP/J001325/1), Leverhulme Trust (RPG-2014-148), University of St Andrews and the MEXT/JSPS Grants in Aid for Scientific Research (JP25102005 and JP25102001) for funding; Simon Barrett for assistance with NMR; Martin Huscroft for assistance with HPLC; and Stephen Boyer for elemental analysis measurements.

Conflict of interest

The authors declare no conflict of interest.

Keywords: cage compounds · homochiral self-sorting · iridium · phosphorescence · supramolecular chemistry

- [1] For reviews, see: a) S. Zarra, D. M. Wood, D. A. Roberts, J. R. Nitschke, *Chem. Soc. Rev.* **2015**, *44*, 419–432; b) T. R. Cook, Y.-R. Zheng, P. J. Stang, *Chem. Rev.* **2013**, *113*, 734–777; c) K. Harris, M. Fujita, *Chem. Commun.* **2013**, *49*, 6703–6712; d) M. D. Ward, *Chem. Commun.* **2009**, 4487–4499; e) D. Fiedler, D. H. Leung, R. G. Bergman, K. N. Raymond, *Acc. Chem. Res.* **2005**, *38*, 349–358.
- [2] For examples and reviews, see: a) J. R. Piper, L. Cletheroe, C. G. P. Taylor, A. J. Metherell, J. A. Weinstein, I. V. Sazanovich, M. D. Ward, *Chem. Commun.* **2017**, *53*, 408–411; b) A. Schmidt, M. Hollering, M. Drees, A. Casini, F. E. Kühn, *Dalton Trans.* **2016**, *45*, 8556–8565; c) L. Xu, Y.-X. Wang, H.-B. Yang, *Dalton Trans.* **2015**, *44*, 867–890; d) X. Yan, T. R. Cook, P. Wang, F. Huang, P. J. Stang, *Nat. Chem.* **2015**, *7*, 342–348; e) J. E. M. Lewis, A. B. S. Elliot, C. J. McAdam, K. C. Gordon, J. D. Crowley, *Chem. Sci.* **2014**, *5*, 1833–1843; f) Z. Li, N. Kishi, K. Yoza, M. Akita, M. M. Yoshizawa, *Chem. Eur. J.* **2012**, *18*, 8358–8365; g) K. Harano, S. Hiraoka, M. Shionoya, *J. Am. Chem. Soc.* **2007**, *129*, 5300–5301; h) N. K. Al-Rasbi, C. Sabatini, F. Barigelletti, M. D. Ward, *Dalton Trans.* **2006**, 4769–4772.

- [3] a) A. Schmidt, M. Hollering, J. Han, A. Casini, F. E. Kühn, *Dalton Trans.* **2016**, 45, 12297–12300; b) A. B. S. Elliott, J. E. M. Lewis, H. van der Salm, C. J. McAdams, J. D. Crowley, K. C. Gordon, *Inorg. Chem.* **2016**, 55, 3440–3447; c) W. J. Ramsay, J. A. Foster, K. L. Moore, T. K. Ronson, R. J. Mirgalet, D. A. Jefferson, J. R. Nitschke, *Chem. Sci.* **2015**, 6, 7326–7331.
- [4] O. Chepelin, J. Ujma, X. Wu, A. M. Z. Slawin, M. B. Pitak, S. J. Coles, J. Michel, A. C. Jones, P. E. Barran, P. J. Lusby, *J. Am. Chem. Soc.* **2012**, 134, 19334–19337.
- [5] a) X. Li, J. Wu, L. Chen, X. Zhong, C. Heng, R. Zhang, C. Duan, *Chem. Commun.* **2016**, 52, 9628–9631; b) X. Li, J. Wu, C. Heng, R. Zhang, C. Duan, *Chem. Commun.* **2016**, 52, 5104–5107.
- [6] a) C. Shen, A. D. W. Kennedy, W. A. Donald, A. M. Torres, W. S. Price, J. E. Beves, *Inorg. Chim. Acta* **2017**, 458, 122–128; b) J. Yang, M. Bhadbhade, W. A. Donald, H. Iranmanesh, E. G. Moore, H. Yan, J. E. Beves, *Chem. Commun.* **2015**, 51, 4465–4468; c) A. B. Wragg, A. J. Metherell, W. Cullen, M. D. Ward, *Dalton Trans.* **2015**, 44, 17939–17949; d) K. Li, L.-Y. Zhang, C. Yan, S.-C. Wei, M. Pan, L. Zhang, C.-Y. Su, *J. Am. Chem. Soc.* **2014**, 136, 4456–4459.
- [7] a) D. Rota Martir, A. K. Bansal, V. Di Mascio, D. B. Cordes, A. F. Henwood, A. M. Z. Slawin, P. C. J. Kamer, L. Martínez-Sarti, A. Pertegás, H. J. Bolink, I. D. W. Samuel, E. Zysman-Colman, *Inorg. Chem. Front.* **2016**, 3, 218–235; b) A. M. Bünzli, E. C. Constable, C. E. Housecroft, A. Prescimone, J. A. Zampese, G. Longo, L. Gil-Escrig, A. Pertegás, E. Ortí, H. J. Bolink, *Chem. Sci.* **2015**, 6, 2843–2852; c) S. Ladouceur, E. Zysman-Colman, *Eur. J. Inorg. Chem.* **2013**, 2985–3007; d) Y. You, S. Y. Park, *Dalton Trans.* **2009**, 1267–1282; e) S. Lamansky, P. Djurovich, D. Murphy, F. Abdel-Razzaq, H. E. Lee, C. Adachi, P. E. Burrows, S. R. Forrest, M. E. Thompson, *J. Am. Chem. Soc.* **2001**, 123, 4304–4312.
- [8] a) A. Schaly, Y. Rousselin, J.-C. Chambron, E. Aubert, E. Espinosa, *Eur. J. Inorg. Chem.* **2016**, 832–843; b) J. J. Henkelis, C. J. Carruthers, S. E. Chambers, R. Clowes, A. I. Cooper, J. Fisher, M. J. Hardie, *J. Am. Chem. Soc.* **2014**, 136, 14393–14396; c) Z. Zhong, A. Ikeda, S. Shinkai, S. Sakamoto, K. Yamaguchi, *Org. Lett.* **2001**, 3, 1085–1087.
- [9] CCDC 1486233 contains the supplementary crystallographic data for this paper. These data are provided free of charge by The Cambridge Crystallographic Data Centre.
- [10] a) C.-T. Wang, L.-C. Shiu, K.-B. Shiu, *Chem. Eur. J.* **2015**, 21, 7026–7029; b) V. Chandrasekhar, T. Hajra, J. K. Bera, S. M. W. Rahaman, N. Satumtira, O. Elbjairami, M. A. Omary, *Inorg. Chem.* **2012**, 51, 1319–1329; c) E. Baranoff, I. Jung, R. Scopelliti, E. Solari, M. Grätzel, Md. K. Nazeeruddin, *Dalton Trans.* **2011**, 40, 6860–6867; d) W.-S. Sie, G.-H. Lee, K. Y.-D. Tsai, I.-J. Chang, K.-B. Shiu, *J. Mol. Struct.* **2008**, 890, 198–202.
- [11] Although NMR spectra of (\pm)-L1 remain unchanged with time, small additional peaks appear in the ^1H NMR spectra of CD_3NO_2 solutions of resolved L1 at room temperature (Figure S2 in the Supporting Information). This may be due to an unknown minor decomposition or saddle-like conformation from crown-saddle-crown racemisation; see for example: G. Huber, T. Brotin, L. Dubois, H. Desvieux, J.-P. Dutasta, P. Berthault, *J. Am. Chem. Soc.* **2006**, 128, 6239–6246.
- [12] J. J. Henkelis, J. Fisher, S. L. Warriner, M. J. Hardie, *Chem. Eur. J.* **2014**, 20, 4117–4125.
- [13] a) P. Bonakdarzadeh, F. Pan, E. Kalenius, O. Jurček, K. Rissanen, *Angew. Chem. Int. Ed.* **2015**, 54, 14890–14893; *Angew. Chem.* **2015**, 127, 15103–15106; b) D. L. Caulder, R. E. Powers, T. N. Parac, K. N. Raymond, *Angew. Chem. Int. Ed.* **1998**, 37, 1840–1843; *Angew. Chem.* **1998**, 110, 1940–1943; c) J. L. Bolliger, A. M. Belenguer, J. R. Nitschke, *Angew. Chem. Int. Ed.* **2013**, 52, 7958–7962; *Angew. Chem.* **2013**, 125, 8116–8120; d) T. Liu, Y. Liu, W. Xuan, Y. Cui, *Angew. Chem. Int. Ed.* **2010**, 49, 4121–4124; *Angew. Chem.* **2010**, 122, 4215–4218; e) S. P. Argent, T. Riis-Johannessen, J. C. Jeffery, L. P. Harding, M. D. Ward, *Chem. Commun.* **2005**, 4647–4649.
- [14] a) S. A. Boer, D. R. Turner, *Chem. Commun.* **2015**, 51, 17375–17378; b) L.-L. Yan, C.-H. Tan, G.-L. Zhang, L.-P. Zhou, J.-C. Bünzli, Q.-F. Sun, *J. Am. Chem. Soc.* **2015**, 137, 8550–8555; c) C. Gütz, R. Hovorka, G. Schnakenburg, A. Lützen, *Chem. Eur. J.* **2013**, 19, 10890–10894; d) C. Maeda, T. Kamada, N. Aratani, A. Osuka, *Coord. Chem. Rev.* **2007**, 251, 2743–2752.
- [15] E. Baranoff, E. Orselli, L. Allouche, D. Di Censo, R. Scopelliti, M. Grätzel, M. K. Nazeeruddin, *Chem. Commun.* **2011**, 47, 2799–2801.

 Manuscript received: March 24, 2017

Accepted Article published: March 29, 2017

Final Article published: April 20, 2017